RSC Advances

PAPER

View Article Online
View Journal | View Issue

Cite this: *RSC Adv.*, 2025, **15**, 15476

Nanoarchitectonics of a covalent organic supramolecular cage (COSC) for fluorescent visual detection of macrolides†

Yu-Ming Guan,‡[a] Hang Gao,‡*[ab] Wen-Bo Xu,[a] Peiyang Su,[a] Tingxia Zhou,[c] Ting-Zheng Xie,*[a] Mingjian Wang,[b] Hongguang Luo*[b] and Pingshan Wang*[a]

Received 30th December 2024
Accepted 26th February 2025

DOI: 10.1039/d4ra09077b

rsc.li/rsc-advances

Macrolides, a major group of antibiotic pollutants, have been widely observed in water and sediments. For onsite identification of macrolides in water environments, we designed and synthesized a quadrangular prism-shaped covalent organic supramolecular cage (COSC) *via* an aldol-amine condensation. Multiple hydrogen bonding sites were introduced into the building blocks to increase host–guest interactions. Meanwhile, by introducing a stimuli-sensitive module, TPE, the fluorescence of the supramolecule changes upon encapsulation of the clarithromycin guest which was a type of macrolides. The cage structure was fully characterized using NMR and high-resolution ESI mass spectrometry. The fluorescence recognition process and detection limitations of the cage for clarithromycin were investigated using NMR, UV-vis, and fluorescence spectroscopy. This study expands the application of precisely designed covalent supramolecular cages for monitoring antibiotic-based environmental pollutants.

Antibiotics are gradually being recognized as important emerging contaminants owing to their diversity, potential toxicity and enhancement of bacterial resistance.[1] Among the antibiotics, macrolides have been widely used and often overused in fisheries and animal husbandry.[2] The identification of macrolide antibiotics in pollutants with high selectivity and sensitivity facilitates the accurate monitoring of antibiotic contaminants and the development of timely environmental treatments.[3]

Compared with traditional analytical instruments, molecular fluorescent probes have the advantages of portability, sensitivity, rapidity and real-time on-site detection.[4] However, for complex real-world contaminants, small molecule fluorescent probes are not selective enough because they tend to signal a change in fluorescence that is in response to chemical reactions between certain functional groups or the formation of metal complexes, instead of the whole molecular recognition of the targets.[5–11] Recently, supramolecules have been recognized as ideal candidates for fluorescent sensors owing to their advantages of pre-designable size and shape of the cavity, reversible recognition and structural adaption. During the development of supramolecular chemistry, numerous luminescent hosts with special cavities, such as macrocycles,[12,13] cages,[14,15] and nanomaterials,[16,17] have been reported as sensors or probes for the detection of small organic molecules, anions

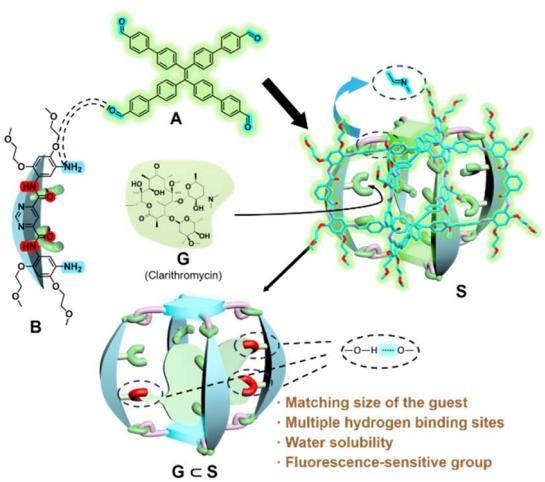

Scheme 1 Construction of the covalent organic fluorescent supramolecular cage S for the detection of clarithromycin contaminants G, the critical design of amine B with multiple guest binding sites and aldehyde A with controllable fluorescence.

[a]*Institute of Environmental Research at Greater Bay Area, Key Laboratory for Water Quality and Conservation of the Pearl River Delta, Ministry of Education, Guangzhou University, Guangzhou 510006, People's Republic of China. E-mail: xietingzheng@gzhu.edu.cn*

[b]*Guangdong Guangye Inspection Testing Group Co., Ltd, Guangzhou, China*

[c]*LIFM, IGCME, School of Chemistry, Sun Yat-Sen University, Guangzhou 510006, China*

† Electronic supplementary information (ESI) available. See DOI: https://doi.org/10.1039/d4ra09077b

‡ Co-first author.

and cations.[18–20] However, the selective detection of larger organic guests, especially antibiotic contaminants in the environment, is relatively challenging[21–24] owing to the large size and structural complexity of antibiotic molecules, which leads to difficulties in the design of the corresponding fluorescent supramolecular hosts. Therefore, to accomplish the sensitive and selective detection of macrolides for further construction of organic pollutant sensors, we designed and synthesized a COSC (denoted as **S**) that was constructed *via* thermodynamically driven condensation of amines with multiple guest binding sites and aldehydes with controllable fluorescence and applied it to the fluorescent sensing of clarithromycin.

According to the structural features of macrolides, taking guest **G** (clarithromycin) as an example, it is composed of a hydrophobic cyclic lactone and two sugar rings containing 12 oxygen atoms and 4 hydroxyl groups, which could be used as binding sites for multiple hydrogen bonds. Based on these molecular features, a diamine module was designed, which contained two amide groups acting as hydrogen bond donor with multiple binding sites for recognizing clarithromycin. The stimuli-sensitive fluorescent moiety of tetraphenylethylene (TPE)[25–27] was designed as a fluorescence indicator because TPE produces fluorescence enhancement or color change when the rotation of the four phenyl groups is affected by steric effects caused by the encapsulation of guests.[28] These two modules are combined by the reaction of aldehyde-amine condensation to form a quadrangular prism-shaped supramolecular cage,[29,30] which encloses a cavity of just the right size to accommodate the clarithromycin guest according to a computer-consisted simulation, which spatially resists the rotation of the two TPE molecules after the guest is captured inside the cavity of the cage, resulting in a change in fluorescence intensity and wavelength. Additionally, since we aim to detect realistic water samples, we introduced glycol chains to the diamine module to improve the water solubility of the supramolecular cage. Therefore, in response to the molecular structural features of clarithromycin guest **G**, we designed a type of supramolecular fluorescent probe for the precise determination of macrolide pollutants by considering the size of supramolecular cage **S**, the multiple hydrogen bonding sites, the solubility, and the fluorescence changes due to the binding of guest **G** (Scheme 1).

A was commercially available as a fluorescent indicator moiety. **B** was synthesized as described in the literature with a critical modification as the macrolide's recognition element. **S** was obtained by combining **A** and **B** in a 1 : 2 ratio for amine-aldehyde condensation catalyzed by trifluoroacetic acid. The [4 + 2] condensation product was fully characterized by ^{1}H, ^{13}C, ^{1}H–^{1}H COSY, NOESY, NMR spectroscopy (Fig. S10–S14†), and HR-ESI-ToF mass spectrometry. All ^{1}H NMR resonances were fully assigned (ESI†).

The ^{1}H NMR spectrum of cage **S** (Fig. 1c) showed one site of peaks, which was consistent with the D_{4h} symmetry of the simulated structure of the quadrangular prism. The comparison of the ^{1}H NMR spectra of cage **S** with the original amines **B** and *tetra* aldehyde **A** (Fig. 1 and S5†) suggested the thorough formation of imine groups owing to the disappearance of the singlet peak at 10.0 ppm assigned to the proton of the aldehyde group.

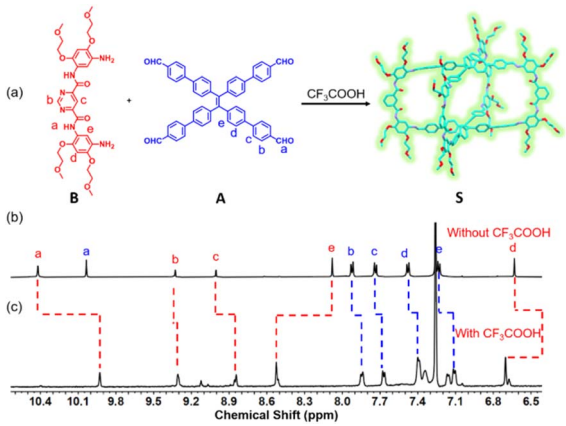

Fig. 1 (a) Synthesis of the supramolecular cage **S**, and the comparison of the ^{1}H NMR spectra of (b) a mixture of ligands **A** and **B** and (c) cage **S**.

The HR-ESI-ToF mass spectrometry provided further evidence for the formation of [4 + 2] cage **S** (Fig. S20†). It showed one dominant set of peaks with continuous charge states from +4 to +2 with the *m*/*z* values of 967.2510, 1289.6642, and 1933.7358, which agreed with the cage but with the loss of one glycol chain. We assumed that the glycol chain might not be sufficiently stable under ESI-MS conditions. Interestingly, the peak at *m*/*z* value of 1933.7358 with charge states of +2 could be assigned to cage **S** losing one **B**, suggesting that one arm of the quadrangular prism may expand to facilitate guest capsulation as a result of the dynamic covalent bond of imines, which are in a reversible equilibrium of disconnection-reformation in cage **S**.

To verify that the well-designed supramolecular cage can be applied for the fluorescent visual determination of macrolides, the inclusion behaviour between the host and guest was studied using ^{1}H NMR, COSY, NOESY, and DOSY spectroscopy (Fig. S6 and S15–S18†). Clarithromycin **G** (10 mg, 12 μmol, 1.5 eq) was added to a $CDCl_3$ solution of cage **S** (1.6×10^{-3} mmol mL^{-1}, 0.5 mL, 1.0 eq) and stirred at room temperature for 30 min. Compared with the ^{1}H NMR spectrum of **G** ⊂ **S** with **G**, it showed a notable upfield shift for the guest signals owing to the shielding effect of the aromatic moieties of cage **S** on **G**, which demonstrated the dynamic encapsulation of clarithromycin **G** by supramolecular cage **S**. The diffusion-ordered NMR spectroscopy (DOSY) showed a single band at diffusion coefficient $D_{(\text{host–guest})} = 6.3 \times 10^{-10}$ m^2 s^{-1}, suggesting that the solution mainly contained a single species and **G** was trapped within the cavity (Fig. S18†). A variable temperature (VT) NMR showed an upfield shift of **G** at 5.2 ppm, and the singlet was split into multiple peaks (Fig. S19 and S20†), indicating that the interactions of **G** ⊂ **S** became more stable as the temperature increased on the NMR time scale. The interactions containing C–H···π and C–H···O between **S** and **G** were also proved by the DFT calculations (Fig. S29†).

Upon the addition of clarithromycin **G** to a $CHCl_3$ solution of cage **S**, the fluorescence of the solution turned blue under 365 nm UV light, which led us to further investigate the

photophysical properties during the recognition of the host–guest. Subsequently, UV/vis experiments were performed for further fluorescence emission studies. Through UV titration, the equilibrium constant was calculated to be 279.46 (Fig. S26†). We added a solution of guest **G** with different concentrations ($CHCl_3$, 10^{-6}, 10^{-5}, 10^{-4}, and 10^{-3} mmol mL^{-1}) to the solution of **S** ($CHCl_3$/MeOH v/v = 1 : 1, 10^{-5} mmol mL^{-1}) and tested their fluorescence using 290 nm as the excitation wavelength (Fig. 2a and S28†). The fluorescence gradually became weaker along with the increase in the concentration of pollutant guest **G**, which was accompanied by a fluorescence colour change from bright green to blue in solution with naked eyes under 365 nm UV light (Fig. 2b and S25†). In the fluorescence spectra, the emission intensity of **S** at 545 nm gradually decreased from 84 673 to 11 972 by adding **G** (10^{-6}–10^{-3} mmol mL^{-1}). The mechanism of the fluorescence quenching effect was attributed to the intermolecular electron transfer of the combination between the multiple hydrogen binding sites of the cage with the encapsulated clarithromycin in the cavity.[31,32]

To demonstrate that **S** can be used for the fast detection analysis of macrolides, we prepared test papers by dipping the filter paper in a solution of **S** at a concentration of 10^{-5} mol L^{-1}. Afterwards, these test papers were tested under four different concentrations of **G** (10^{-6}–10^{-3} mmol mL^{-1}). The images of test papers under 365 nm UV light showed that the colour of fluorescence changed significantly fluorescence quenching from bright green to blue (the original colour of the test paper) as the concentration increased (Fig. 2b). The LOD of **S** for clarithromycin was calculated to be 80 ppb (Fig. S24†), which is similar to the results of the instrumental analysis.[33] Fluorescence measurements were performed for three other macrolides, namely, fidaxomicin, dirithromycin, and azithromycin. The data showed that **G** had the greatest change at a maximum wavelength of 545 nm in fluorescence (Fig. S27†), suggesting the competitive selectivity of cage **S** for clarithromycin **G**.

In conclusion, to construct a suitable supramolecular cage with specific fluorescent recognition of macrolides, we designed and synthesized a type of quadrangular prism-shaped, imine-based COSC by incorporating four factors into the design of supramolecular cage fluorescent probes: a cavity matching the size of the guest molecule, multiple hydrogen bonding sites for enhanced host–guest interactions, solubility compatible with the aqueous environment, and a fluorescence-sensitive group for generating fluorescence changes. The encapsulation of clarithromycin in the cavity of the cage was clearly characterized by ^{1}H NMR spectra, in which the intermolecular charge transfer effect led to significant fluorescent quenching that can be observed by the naked eye. On the determination of the clarithromycin, it exhibits perceptible fluorescence extinction with an LOD of 80 ppb. The results showed that supramolecular cages can be designed for the molecular structure of environmental pollutants as highly selective and sensitive fluorescent probes.

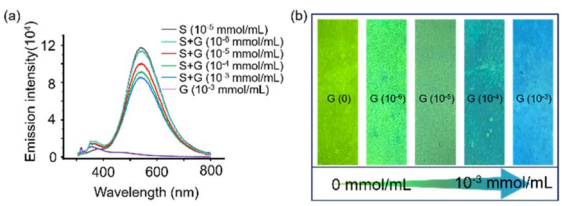

Fig. 2 (a) Fluorescence spectra of **G** with different concentrations added to **S** (10^{-5} mol L^{-1}). (b) Images of test papers dipped with **S** (10^{-5} mmol mL^{-1}) in different concentrations of **G** under 365 nm UV light.

Data availability

The authors confirm that the data supporting the findings of this study are available within the article and/or its ESI.†

Author contributions

The synthesis of the organic ligands and supramolecular cage and the NMR spectra experiments were conducted by Yu-Ming Guan. The data generation and analysis were done by Dr Gao. She also provided ideas for commercialization of this on-site testing method. The fluorescence test was done by Wen-Bo Xu.

Conflicts of interest

There are no conflicts to declare.

Acknowledgements

This research was supported by the National Natural Science Foundation of China (21971257 to P. W., 21971048 to T.-Z. X.), the Guangdong Provincial Pearl River Talents Program (2019QN01C24 to T.-Z. X.), the Technical Cooperation Project between Guangzhou University and Guangdong Guangye Inspection & Testing Group Co., Ltd. (No. GK2023097).

References

1 A. Tarai, Y. Li, B. Liu, D. Zhang, J. Li, W. Yan, J. Zhang, J. Qu and Z. Yang, *Coord. Chem. Rev.*, 2021, **445**, 214070.
2 A. C. Pawlowski, P. J. Stogios, K. Koteva, T. Skarina, E. Evdokimova, A. Savchenko and G. D. Wright, *Nat. Commun.*, 2018, **9**, 112.
3 N. A. Nor Amdan, N. A. Shahrulzamri, R. Hashim and N. Mohamad Jamil, *J. Global Antimicrob. Resist.*, 2024, **38**, 368–375.
4 T. L. Mako, J. M. Racicot and M. Levine, *Chem. Rev.*, 2018, **119**, 322–477.
5 S. Chanmungkalakul, V. Ervithayasuporn, P. Boonkitti, A. Phuekphong, N. Prigyai, S. Kladsomboon and S. Kiatkamjornwong, *Chem. Sci.*, 2018, **9**, 7753–7765.
6 N. Oguri, Y. Egawa, N. Takeda and M. Unno, *Angew. Chem., Int. Ed.*, 2016, **55**, 9336–9339.
7 B. M. Chapin, P. Metola, S. L. Vankayala, H. L. Woodcock, T. J. Mooibroek, V. M. Lynch, J. D. Larkin and E. V. Anslyn, *J. Am. Chem. Soc.*, 2017, **139**, 5568–5578.

8 C. Guo, A. C. Sedgwick, T. Hirao and J. L. Sessler, *Coord. Chem. Rev.*, 2021, **427**, 213560.
9 A. J. Plajer, E. G. Percástegui, M. Santella, F. J. Rizzuto, Q. Gan, B. W. Laursen and J. R. Nitschke, *Angew. Chem., Int. Ed.*, 2019, **58**, 4200–4204.
10 T. K. Ronson, S. Zarra, S. P. Black and J. R. Nitschke, *Chem. Commun.*, 2013, **49**, 2476–2490.
11 T. Uchida, Y. Egawa, T. Adachi, N. Oguri, M. Kobayashi, T. Kudo, N. Takeda, M. Unno and R. Tanaka, *Chem.–Eur. J.*, 2019, **25**, 1683–1686.
12 L. E. Kreno, K. Leong, O. K. Farha, M. Allendorf, R. P. Van Duyne and J. T. Hupp, *Chem. Rev.*, 2012, **112**, 1105–1125.
13 Y. Cui, B. Chen and G. Qian, *Coord. Chem. Rev.*, 2014, **273–274**, 76–86.
14 M. R. Hamblin, *Photochem. Photobiol. Sci.*, 2018, **17**, 1515–1533.
15 J. J. Henkelis and M. J. Hardie, *Chem. Commun.*, 2015, **51**, 11929–11943.
16 B. Yan, *Acc. Chem. Res.*, 2017, **50**, 2789–2798.
17 Y. Zhang, S. Yuan, G. S. Day, X. Wang, X. Yang and H. Zhou, *Coord. Chem. Rev.*, 2018, **354**, 28–45.
18 J. Schütt, B. Ibarlucea, R. Illing, F. Zörgiebel, S. Pregl, D. Nozaki, W. M. Weber, T. Mikolajick, L. Baraban and G. Cuniberti, *Nano Lett.*, 2016, **16**, 4991–5000.
19 J. Krämer, R. Kang, L. M. Grimm, L. De Cola, P. Picchetti and F. Biedermann, *Chem. Rev.*, 2022, **122**, 3459–3636.
20 S. Chatterjee and A. R. Paital, *Adv. Funct. Mater.*, 2018, **28**, 1704726.
21 A. P. Davis, *Chem. Soc. Rev.*, 2020, **49**, 2531–2545.
22 W. Liu, S. Bobbala, C. L. Stern, J. E. Hornick, Y. Liu, A. E. Enciso, E. A. Scott and J. F. Stoddart, *J. Am. Chem. Soc.*, 2020, **142**, 3165–3173.
23 W. Liu and J. F. Stoddart, *Chem*, 2021, **7**, 919–947.
24 S. Saha, B. Kauffmann, Y. Ferrand and I. Huc, *Angew. Chem., Int. Ed.*, 2018, **57**, 13542–13546.
25 J. Gu, W. Yuan, K. Chang, C. Zhong, Y. Yuan, J. Li, Y. Zhang, T. Deng, Y. Fan, L. Yuan, S. Liu, Y. Xu, S. Ling, C. Li, Z. Zhao, Q. Li, Z. Li and B. Z. Tang, *Angew. Chem., Int. Ed.*, 2025, **64**, e202415637.
26 W.-J. Wang, R. Zhang, L. Zhang, L. Hao, X.-M. Cai, Q. Wu, Z. Qiu, R. Han, J. Feng, S. Wang, P. Alam, G. Zhang, Z. Zhao and B. Z. Tang, *Nat. Commun.*, 2024, **15**, 9999.
27 S. Xue, Z. Shi, Z. Wang, H. Tan, F. Gao, Z. Zhang, Z. Ye, S. Nian, T. Han, J. Zhang, Z. Zhao, B. Z. Tang and Q. Zhang, *Nat. Commun.*, 2024, **15**, 10084.
28 S. Jung, J. Park, J. Bang, J.-Y. Kim, C. Kim, Y. Jeon, S. H. Lee, H. Jin, S. Choi, B. Kim, W. J. Lee, C.-G. Pack, J.-B. Lee, N. K. Lee and S. Kim, *J. Am. Chem. Soc.*, 2017, **139**, 7603–7615.
29 X. Zhao, H. Cui, L. Guo, B. Li, J. Li, X. Jia and C. Li, *Angew. Chem., Int. Ed.*, 2024, **63**, e202411613.
30 M. Asad, M. Imran Anwar, A. Abbas, A. Younas, S. Hussain, R. Gao, L.-K. Li, M. Shahid and S. Khan, *Coord. Chem. Rev.*, 2022, **463**, 214539.
31 T. Cheng, D. X. Shen, M. Meng, S. Mallick, L. Cao, N. J. Patmore, H. L. Zhang, S. F. Zou, H. W. Chen, Y. Qin, Y. Y. Wu and C. Y. Liu, *Nat. Commun.*, 2019, **10**, 1531.
32 H. S. S. Ramakrishna Matte, K. S. Subrahmanyam, K. Venkata Rao, S. J. George and C. N. R. Rao, *Chem. Phys. Lett.*, 2011, **506**, 260–264.
33 R. A. Pérez, B. Albero, M. Férriz and J. L. Tadeo, *J. Pharm. Biomed. Anal.*, 2017, **146**, 79–85.